MUSCLE CONTRACTION INDUCES OSTEOGENIC LEVELS OF CORTICAL BONE STRAIN DESPITE MUSCLE WEAKNESS IN A MOUSE MODEL OF OSTEOGENESIS IMPERFECTA

Alycia G. Berman,[a] Jason M. Organ, Ph.D.,[b] Matthew R. Allen, Ph.D,[b,c] and Joseph M. Wallace, Ph.D.[c]

[a] Weldon School of Biomedical Engineering,
Purdue University, West Lafayette, IN, USA
[b] Department of Anatomy and Cell Biology,
Indiana University School of Medicine, Indianapolis, IN, 46202
[c] Department of Biomedical Engineering,
Indiana University-Purdue University at Indianapolis, Indianapolis, IN, USA

Corresponding Author:
Joseph M. Wallace, Ph.D.
Department of Biomedical Engineering
Indiana University-Purdue University at Indianapolis
Indianapolis, IN, USA
jmwalla@iupui.edu
+1-317-274-2448

Funding Sources: This work was supported by the NIH (AR067221 to J.M.W.) and the NSF (DGE-1333468 to A.G.B.).

Supplementary Data: Text and one figure included.

This is the author's manuscript of the article published in final edited form as:

Berman, A. G., Organ, J. M., Allen, M. R., & Wallace, J. M. (2020). Muscle contraction induces osteogenic levels of cortical bone strain despite muscle weakness in a mouse model of Osteogenesis Imperfecta. Bone, 132, 115061. https://doi.org/10.1016/j.bone.2019.115061

Abstract

Mechanical interactions between muscle and bone have long been recognized as integral to bone integrity. However, few studies have directly measured these interactions within the context of musculoskeletal disease. In this study, the osteogenesis imperfecta murine model (oim/oim) was utilized because it has both reduced bone and muscle properties, allowing direct assessment of whether weakened muscle is able to engender strain on weakened bone. To do so, a strain gauge was attached to the tibia of healthy and oim/oim mice, muscles within the posterior quadrant of the lower hind limb were stimulated, and bone strain during muscle contraction was measured. Results indicated that the relationship between maximum muscle torque and maximum engendered strain is altered in oim/oim bone, with less torque required to engender strain compare to wild-type and heterozygous mice. Maximum muscle torque at 150 Hz stimulation frequency was able to engender ~1500 με in oim/oim animals. However, even though the strain engendered in the oim/oim mice was high relative to historical bone formation thresholds, the maximum strain values were still significantly lower than that of the wild-type mice. These results are promising in that they suggest that muscle stimulation may be a viable means of inducing bone formation in oim/oim and potentially other disease models where muscle weakness/atrophy exist.

Keywords: Bone-muscle interactions, Biomechanics, Exercise, Osteogenesis imperfecta, Sarcopenia

1. Introduction

Muscle and bone are intricately linked, both physically and chemically. From a strictly mechanical perspective, muscles attach to bone and use these bone attachment sites as the lever arms by which they enable movement. In fact, the relatively small distance between the muscle attachment site and the joint creates an unfavorable lever arm, implying that during movement, the muscle must exert a much larger force on bone compared to ground reaction forces. Lu et al. found that less than 30% of the forces transmitted through the femur during normal gait were derived from the ground reaction force, with a much higher 70% driven from muscle contraction.[1] Similarly, Wehner et al. calculated the internal loads in the human tibia during gait and found that the forces were up to 4.7 times the body weight.[2] For this reason, some have suggested that muscle may be a primary means of mechanically stimulating bone.[3]

Mechanical loading has been well-established as integral to maintaining bone integrity. Below a strain threshold, bone loss will occur while above a different strain threshold, bone formation will occur.[4,5] Given the importance of mechanical loading to bone health, and considering the ability of muscle to engender significant forces on bone, it follows that muscle health is likely also critical to bone health. Indeed, correlative relationships between muscle and bone have been well-documented.[6,7] For example, in situations of long-term bedrest, low bone mass and poor muscle tone occur together.[8] Similarly, osteoporosis is often associated with sarcopenia.[9,10] A number of studies have even shown that skeletal muscle mass can be a predictor of bone mass[11] or bending stiffness.[12] Interestingly, these correlations also occur with genetic diseases that primarily impact only one aspect of the musculoskeletal system (i.e. directly impacting only bone or only muscle).

Osteogenesis Imperfecta (OI) is a bone disease driven by a mutation to the genes involved in the Type I collagen synthesis pathway.[13] Patients with OI show skeletal weakness,

ranging from mild to severe to perinatal lethal.[14] Despite OI being considered a "bone disease," muscle is often also impacted in OI patients,[15-18] with the degree of impact dependent on the severity of the disease.[19] In the preclinical realm, one commonly used mouse model of OI is the Osteogenesis Imperfecta Murine (oim/oim) model. Oim/oim results from a single G nucleotide deletion in the COL1A2 gene. This change causes a frameshift in the final 48 amino acids at the C terminus, resulting in an extra amino acid which renders the α2 chain non-functional. The end result is the accumulation of homotrimeric collagen instead of the normal heterotrimeric molecule.[20] In its homozygous form, oim/oim mice show significant skeletal weakness and spontaneous fractures, while the heterozygous form is milder.[20-24] Also similar to the human condition, oim/oim mice have muscular weakness.[25] In the homozygous mice, muscle size and strength are significantly reduced, while the heterozygous mice show a milder, non-significant reduction.[25]

Given that muscle and bone are both impacted by OI, it is unclear how efficiently weakened muscle is able to engender strain on the bone. In other words, if only muscle were affected, then weaker muscle would imply lower forces (and thereby lower strain) on bone. In contrast, if only bone were affected, then the muscle force would remain the same, but the bone strain would presumed to be increased because the bone is weaker. To address this uncertainty, we attached a strain gauge to the anteromedial mid-diaphysis of the tibia of both wild-type and oim/oim mice and then conducted *in vivo* muscle stimulation to induce plantar flexion. This setup enabled us to collect muscle ankle torque and bone strain simultaneously. In addition, *ex vivo* morphological analyses of bone and muscle by micro-computed tomography (CT) were used to assess bone mass and muscle area. Our hypothesis was that the muscle-bone unit would find an equilibrium such that engendered bone strain would be conserved across mouse strains.

2. Methods

2.1 Experimental Overview

Wild-type (WT), heterozygous (Het), and homozygous (oim/oim) oim mice were bred in-house and maintained on a C57BL/6J background.[26] Mice were group housed in a facility with 12-hour light/dark cycles and access to food and water *ad libitum*. At 16 weeks of age, male mice (n= 7-9/group; Table 1) from each genotype underwent surgery to attach a strain gauge to the anteromedial portion of the mid-diaphysis of the right tibia. After attachment of the gauge, but while still under anesthesia, the mouse was moved to a muscle testing machine and the tibial nerve was stimulated to induce plantarflexion. After collection of torque and strain data, the mouse was euthanized. The strain gauge was manually checked to ensure firm attachment, and then the right limb was dissected out, wrapped in saline, and stored at -20 °C until imaging by micro-computed tomography (micro-CT). This initial imaging session was used to assess any obvious bone abnormalities (broken or bent bones, etc.) and to estimate muscle cross-sectional area. Soft tissue was then dissected away, and the tibia was imaged again by micro-CT for bone structural information. All procedures were conducted with prior approval from Indiana University School of Medicine IACUC.

2.2 Strain Gauge Attachment

Mice were anesthetized with 1-3% isoflurane and chemical depilatory cream was applied to the lower right hind limb to remove hair. An incision was then made through the skin and fascia, exposing the anteromedial portion of the midshaft tibia. The surface of the bone was degreased, and a single-element strain gauge with gauge dimensions of 2.54 mm L x 0.51 mm W (EA-06-015DJ-120, Vishay Precision Group, Shelton, CT) was aligned with the long axis of the tibia and attached using a cyanoacrylate-based adhesive (Loctite Super Glue, Henkel-Adhesives,

Düsseldorf, Germany). During strain measurement, the gauge was attached to a strain gauge conditioner (2100 Signal Conditioning Amplifier System, Micro-Measurements, Vishay Precision Group, Shelton, CT) via a quarter-bridge completion. Calibration to ensure accurate conversion from volts to strain was performed by adjusting the signal gain based on the gauge factor, per manufacturer instructions.

2.3 Muscle Stimulation

Isometric muscle stimulation was performed using an *in vivo* setup (Aurora Scientific Inc., Ontario, Canada). The mouse's foot was taped to the machine's footplate (a torque transducer) which was used to measure ankle torque during plantarflexion. Two sterile shielded monopolar needle electrodes were inserted on either side of the tibial nerve, slightly proximal to the mid-calf level, and were adjusted to ensure maximum twitch response. This setup of the electrodes primarily stimulates the gastrocnemius and soleus muscles to induce plantarflexion, but also has some contributions from the plantaris, flexor hallucis longus, flexor digitorium longus, and tibialis posterior. The muscles were then stimulated (0.5 msec pulse width), beginning at 25 Hz and extending to 300 Hz in 25-Hz increments. The muscles were stimulated at each frequency for 200 msec, followed by 45 seconds of rest before moving to the next frequency. During stimulation, both muscle torque and bone strain were recorded (Figure 1). Data were analyzed using a custom Matlab script to determine maximum torque and strain at each stimulation frequency. In addition, the torque-time slope at each stimulation frequency was calculated by fitting a linear regression to the maximum rising slope of each torque-time graph.

2.4 Micro-Computed Tomography (micro-CT)

Whole right limbs were scanned by high resolution micro-CT (Skyscan 1176; Bruker, Kontich, Belgium) at an 8.4 μm resolution (V = 50 kV; I = 500 μA; Step size = 0.9°; no

averaging).[27] Projection images were used to assess the presence of broken bones and/or calcified tendon. After reconstruction and rotation, a 1-mm region of interest at the tibial mid-diaphysis was used to estimate total soft-tissue volume and bone volume. These volumes were converted to averaged areas by dividing the volume by the length of the region of interest (1 mm). Muscle area was then calculated as the difference between the total soft-tissue area and the area of the bone and marrow.

The soft tissue was then removed in order to acquire a more crisp image set, and the tibia was scanned again by high resolution micro-CT (Skyscan 1172; Bruker, Kontich, Belgium) using the following parameters: 10 μm resolution, 60 kV tube voltage, 167 μA current, 0.7-degree increment angle, and 2-frame averaging. To convert gray-scale images to mineral content, hydroxyapatite calibration phantoms (0.25 and 0.75 g/cm3 CaHA) were also scanned. After reconstruction and rotation (nRecon and DataViewer, Bruker), 1-mm regions of interest were selected in the proximal metaphysis (Supplemental Text and Figure 1) and mid-diaphysis for analysis. In the mid-diaphysis, the cortical shaft was analyzed using a custom Matlab script (MathWorks, Inc. Natick, MA) to determine areas (total cross sectional area and marrow area), periosteal and endocortical bone surface, maximum principal moment of inertia, and tissue mineral density.

2.5 Statistical Analysis

All statistics were performed in Prism (Graphpad Software, San Diego, CA). For torque and strain data, a two-way ANOVA was performed to assess the main effects of stimulation frequency and genotype. A post-hoc Tukey HSD test was then performed at each stimulation frequency to assess individual differences between genotypes ($p<0.05$). For CT data, we used a one-way ANOVA with a post-hoc Tukey HSD test to determine effects of genotype ($p<0.05$).

For the strain-torque regression, a linear regression was used to assess correlations between variables. Comparison of the linear regression slopes was assessed by ANCOVA with post-hoc Tukey HSD test ($p<0.05$). All data are presented as mean ± standard deviation.

3. Results

3.1 General Animal Information

Animal numbers for each group are shown in Table 1. One oim/oim mouse had a broken right tibia at the time of surgery and one Het mouse showed a large area of woven bone. Both were excluded from all analysis. In addition, difficulties with strain gauge attachment such as a non-secure gauge, off-axis placement, or a break in the wire or gauge precluded some mice from strain analysis (Table 1). Note that the mice with strain gauge attachment errors were still included in other analyses (micro-CT and muscle torque).

Table 1: Number of animals per group

	WT	**HET**	**OIM**
Initial Group Numbers	8	9	7
Broken Tibia or Woven Bone (excluded from all analysis)	0	1	1
Poor Strain Gauge Placement (excluded from strain)	3	2	2

A significant difference in body weight was noted for oim/oim (18.7±2.6 g) compared to both Het (28.4±2.1 g; $p<0.001$) and WT (28.4±1.7 g; $p<0.001$) mice. Tibial length was also significantly lower in oim/oim (16.2±0.8 mm) compared to Het (17.8±0.4 mm; $p<0.001$) and WT (18.1±0.2 mm; $p<0.001$). There were no significant differences in weight or tibial length between WT and Het.

3.2 Muscle Contractile Force and Cross Sectional Area

Measurements of maximum torque at each stimulation frequency showed significant muscle weakness in oim/oim in all but the lowest stimulation frequency (Figure 2A). To further explore maximum torque during tetanic contraction, data was plotted at the 150 Hz stimulation frequency (Figure 2B-C). Maximum torque was significantly lower in oim/oim by 77% ($p<0.001$) and 74% ($p<0.001$) compared to the WT and Het, respectively (Figure 2B). There was also a marked suppression in the rising slope of the torque-time curves in the Het compared to the WT ($p=0.03$) and in the oim/oim compared to both the WT ($p<0.001$) and Het ($p<0.001$) (Figure 2C). Similar to the functional muscle assessment, muscle cross-sectional area estimated by micro-CT indicated that oim/oim had 46% ($p<0.001$) and 49% ($p<0.001$) less muscle area compared to WT and Het (Figure 2D). No significant differences were noted between WT and Het for any muscle parameters.

3.3 Cortical Bone Structural Parameters

Oim/oim mice also had significantly smaller bones compared to both WT and Het (Figure 3A-C). Oim/oim showed a 24% lower cross-sectional area compared to both WT and Het (both $p<0.01$; Figure 3D). A similar difference was observed in marrow area (-22% vs WT, -19% vs Het; both $p<0.01$; Figure 3E). Measurements of periosteal and endocortical perimeters corroborated these results, with both showing significantly smaller values in oim/oim mice (Figure 3G-H). This smaller geometry led to 43% and 46% lower maximum moment of inertia in oim/oim compared to WT ($p<0.05$) and Het ($p<0.01$), respectively (Figure 3F). Similarly, minimum moment of inertia was 45% and 43% lower in oim/oim compared to WT ($p<0.01$) and Het ($p<0.01$), respectively. Interestingly, oim/oim had significantly higher tissue mineral density than WT ($p<0.01$) and Het ($p<0.05$), suggesting increased mineralization (Figure 3I). No significant differences were noted between WT and Het for any cortical parameters.

3.4 Bone Strain and Torque-Strain Interaction

Despite the significant muscle weakness noted in the oim/oim mice, the engendered tensile strain during maximum tetanic contraction at the 150 Hz stimulation frequency was 1488±416 με, which is within the range of strains shown to induce a bone formation response in this age of mouse.[4,5] This value was 41% lower compared to WT ($p=0.03$). Het values of strain induced at 150 Hz were intermediate and not significantly different from either WT or oim/oim (Figure 4B). Similar results were observed at the other frequencies, with all but the lowest two frequencies showing significantly lower strain in the oim/oim mice compared to wild-type mice at a matched frequency (Figure 4A).

To further demonstrate the relationship between bone and muscle, bone strain per unit of muscle torque was calculated. Oim/oim had significantly higher strain per torque compared to both WT and Het at all frequencies (Figure 4C). At 150 Hz stimulation frequency, oim/oim had a 441% greater ratio than WT and a 558% greater ratio than Het (both $p<0.001$; Figure 4D). Similarly, when all stimulation frequencies and mice were plotted to examine correlations between strain and torque (Figure 4E), oim/oim had a significantly steeper slope than either WT or Het (both $p<0.001$).

3.5 Tendon Calcification and Broken Calcaneus

As assessed by CT (Figure 5), oim/oim had the greatest number of mice with calcification of the Achilles tendon, though calcification was also observed in some Het. In addition, over half of the oim/oim had a broken right calcaneus, with large callus formation indicating a fracture that had occurred before the muscle stimulation and that had started to heal. These mice (n=4) had 76% lower maximum muscle torque than oim/oim with intact calcaneus (n=2). Given that the transmission of force from the muscle goes through the tendon and

calcaneus, the tendon and calcaneus are likely important contributors to muscle-bone interactions.

4. Discussion

Mechanical interactions between muscle and bone have long been recognized as integral to bone integrity. However, few studies have directly measured these interactions within the context of musculoskeletal disease. In this study, we attached a strain gauge to the tibia of healthy and OI mice and measured bone strain during muscle contraction. Our primary results showed that oim/oim muscle was able to engender an average of ~1500 με on bone despite muscle weakness. Even so, this strain value was significantly lower than the ~2500 με engendered by WT mice.

The first finding was that the oim/oim mice required less muscle torque to engender a given bone strain, as may be expected given the reduction in bone properties observed in this model. Previous studies have shown that oim/oim have reduced bone mass and bone mechanical properties, including stiffness.[24,28-30] Although we did not measure mechanical properties in the current study, measurements of cortical and cancellous bone geometry and density (Supplemental Text and Figure 1) indicated that oim/oim animals had significantly smaller bones with a drastically lower cross sectional moment of inertia. Moment of inertia is a measure of a bone's structural ability to resist bending. Therefore, although moment of inertia is not a direct mechanical measurement, a lower moment of inertia would indicate that a bone can more easily deform under a given load, similar to what has been reported previously.

The reduction in bone properties was paired with reductions in estimated muscle cross-sectional area and function. Muscle weakness is often observed clinically,[16-18,31] and can even be considered the presenting sign of OI.[32,33] A study by Veilleux *et. al* showed that OI Type I

patients had lower average peak force, even after normalizing to muscle cross-sectional area. Similar results were noted in the pre-clinical realm, with Gentry *et al.* showing that the maximum contractile force and specific contractile force were lower in the plantaris, gastrocnemius, and tibialis anterior of oim/oim mice.[25] In the current study, oim/oim mice had reduced maximum muscle torque during plantarflexion and lower estimated muscle cross-sectional area.

Despite the significant muscle weakness, and presumably due to oim/oim bone's increased propensity to bending, the strain engendered on the oim/oim bone during maximum muscle contraction was above historical osteogenic strain thresholds,[4,5] suggesting at least partial conservation in the muscle-bone relationship, even in disease. The implication of this is that muscle stimulation, although lower than normal, may be able to mechanically induce bone formation in OI. This idea—using muscle to improve OI bone—has been previously explored. In a study by Oestreich *et al.*, myostatin deficiency in Het mice resulted in improved bone strength.[34] Similarly, administration of a soluble activin receptor 2B to increase muscle mass in Het also increased bone mass.[35] Our study suggests that the improvements to bone may be driven—at least partially—by the mechanical loading of the bone during muscle contraction.

Although strain levels in the oim/oim were high relative to historical osteogenic strain thresholds, they were still lower than WT, suggesting that even at maximum muscle contraction, oim/oim would likely have a reduced bone formation effect. In other words, as Sugiyama et al. demonstrated, the bone's response to mechanical stimulation is linear within the anabolic strain region.[4] Thus, even though the strain level is anabolic in WT, Het, and oim/oim, the bone formation effects would likely be diminished in oim/oim. Similarly, oim/oim may have to exert greater forces relative to their maximum contractile force in order to have a desired effect. This

finding suggests that it may require more "effort" to induce a bone formation response in oim/oim than in WT. For example, if we consider ~1000 με as the threshold for bone formation,[4,5] then a WT mouse—which engenders a maximum of ~2500 με on bone—may only have to exert ~40% of its maximum muscle force in order to be above the strain threshold for bone formation. In contrast, an oim/oim mouse—which only engenders a maximum of ~1500 με on bone—may need to exert nearly 70% of its maximum muscle force to have the same effect. Thus, even though oim/oim had both weaker muscle and weaker bone, the relationship between muscle and bone was not fully conserved in this model in that the oim/oim have to exert more "effort" to obtain the same strain response.

It is also important to note that, during standard locomotion, a person rarely exerts maximum muscle force. We chose muscle stimulation in the current experiment because it afforded greater control over muscle contraction properties, but care must be taken in the interpretation of our data. Maximum contraction during muscle stimulation is much higher than observed during normal activity. For example, strain values during walking in healthy mice have been reported as approximately 200 με of tension,[36] which is much lower than the ~2500 με engendered in the WT mice during maximum muscle contraction. Despite these differences, the fact that maximum muscle stimulation can cause ~1500 με of tensile strain in oim/oim is encouraging, and would suggest an interesting avenue for further exploration.

One important observation in this study was that the Achilles tendon had some calcification in most of the oim/oim and half of the Het animals. Previous work have also noted Achilles tendon calcification in oim/oim,[37,38] and studies of oim/oim tail tendon have indicated that oim/oim had reduced mechanical integrity[39] and altered structure.[40,41] In our study, Het mice with calcification of the tendon as determined by the bright streak in the micro-CT had a

non-significant reduction in maximum muscle torque. In addition, the calcaneus in nearly half of the oim/oim was broken, but the presence of a callus indicates that the break occurred prior to muscle stimulation. As might be expected, the mice with a broken calcaneus had a much lower maximum muscle torque compared to oim/oim with intact bone. Clearly, the tendon and calcaneus are important to force transmission from muscle to bone. Although we did not explore this further, additional research into the role of the tendon and calcaneus are warranted.

A few limitations should be noted. First, this study only assessed mechanical interactions of muscle and bone, and did not explore chemical interactions, even though those are likely impacted as well. A growing body of literature has indicated the importance of muscle-bone molecular and biochemical interactions, as demonstrated by an increased number of reviews on the topic.[42-44] However, we have limited our scope to purely mechanical interactions, as could be assessed by strain gauging. Second, we also used imaging to estimate muscle cross-sectional area, which does not allow us to differentiate skeletal muscle, connective tissue, and adipose. Our estimates show differences among groups that are consistent with previous literature using more traditional histological measures. Lastly, the OI murine model used in this study has an $\alpha 2$ chain mutation, which is less common in humans. In addition, presence of spontaneous fractures in the long bones limits the mice available for studies. Despite these limitations in the mouse model, oim/oim does show both muscle and bone weakness as is common in human patients and is the primary reason this model was chosen.

In summary, we have demonstrated that oim/oim mice require less muscle torque to engender strain on bone. As a result, although the oim/oim have extreme muscle weakness, maximum muscle contraction was still able to engender ~1500 $\mu\varepsilon$. This engendered strain was

still lower in oim/oim than in the WT. Even so, these results are promising in that they show that muscle stimulation induces strains above historical bone formation thresholds in oim/oim.

5. Acknowledgements

We would like to gratefully acknowledge Dr. Charlotte L. Phillips for providing us with the breeders used in this study. This work was supported by the NIH (AR067221 to J.M.W.) and the NSF (DGE-1333468 to A.G.B.).

Authors' roles: Study design: AGB, JMO, MRA, and JMW. Study conduct, data collection, and data analysis: AGB. Data interpretation: AGB and JMW. Drafting, revising, and approving the final manuscript: AGB, JMO, MRA, and JMW. AGB and JMW take responsibility for the integrity of the data analysis.

References:

1. Lu T-W, Taylor SJ, O'Connor JJ, Walker PS. 1997. Influence of muscle activity on the forces in the femur: An in vivo study. J Biomech. 30(11-12):1101-1106.

2. Wehner T, Claes L, Simon U. 2009. Internal loads in the human tibia during gait. Clinical Biomechanics. 24(3):299-302.

3. Robling AG. 2009. Is bone's response to mechanical signals dominated by muscle forces? Med Sci Sports Exerc. 41(11):2044.

4. Sugiyama T, Meakin LB, Browne WJ et al. 2012. Bones' adaptive response to mechanical loading is essentially linear between the low strains associated with disuse and the high strains associated with the lamellar/woven bone transition. J Bone Miner Res. 27(8):1784-1793.

5. Turner CH, Forwood MR, Rho JY, Yoshikawa T. 1994. Mechanical loading thresholds for lamellar and woven bone formation. J Bone Miner Res. 9(1):87-97.

6. Burr DB. 1997. Muscle strength, bone mass, and age-related bone loss. J Bone Miner Res. 12(10):1547-1551.

7. Kaye M, Kusy RP. 1995. Genetic lineage, bone mass, and physical activity in mice. Bone. 17(2):131-135.

8. Rittweger J, Frost HM, Schiessl H et al. 2005. Muscle atrophy and bone loss after 90 days' bed rest and the effects of flywheel resistive exercise and pamidronate: Results from the ltbr study. Bone. 36(6):1019-1029.

9. Sjöblom S, Suuronen J, Rikkonen T et al. 2013. Relationship between postmenopausal osteoporosis and the components of clinical sarcopenia. Maturitas. 75(2):175-180.

10. Verschueren S, Gielen E, O'neill T et al. 2013. Sarcopenia and its relationship with bone mineral density in middle-aged and elderly european men. Osteoporos Int. 24(1):87-98.

11. Blain H, Jaussent A, Thomas E et al. 2010. Appendicular skeletal muscle mass is the strongest independent factor associated with femoral neck bone mineral density in adult and older men. Exp Gerontol. 45(9):679-684.

12. Myburgh KH, Charette S, Zhou L et al. 1993. Influence of recreational activity and muscle strength on ulnar bending stiffness in men. Med Sci Sports Exerc. 25(5):592-596.

13. Gajko-Galicka A. 2002. Mutations in type i collagen genes resulting in osteogenesis imperfecta in humans. ACTA BIOCHIMICA POLONICA-ENGLISH EDITION-. 49(2):433-442.

14. Sillence D, Senn A, Danks D. 1979. Genetic heterogeneity in osteogenesis imperfecta. J Med Genet. 16(2):101-116.

15. Takken T, Terlingen HC, Helders PJ et al. 2004. Cardiopulmonary fitness and muscle strength in patients with osteogenesis imperfecta type i. The Journal of pediatrics. 145(6):813-818.

16. Pouliot-Laforte A, Veilleux LN, Rauch F, Lemay M. 2015. Physical activity in youth with osteogenesis imperfecta type i. J Musculoskelet Neuronal Interact. 15(2):171-176.

17. Veilleux L-N, Lemay M, Pouliot-Laforte A et al. 2014. Muscle anatomy and dynamic muscle function in osteogenesis imperfecta type i. The Journal of Clinical Endocrinology & Metabolism. 99(2):E356-E362.

18. Veilleux L-N, Pouliot-Laforte A, Lemay M et al. 2015. The functional muscle–bone unit in patients with osteogenesis imperfecta type i. Bone. 79:52-57.

19. Engelbert R, Van Der Graaf Y, Van Empelen R, Beemer F, Helders P. 1997. Osteogenesis imperfecta in childhood: Impairment and disability. Pediatrics. 99(2):e3-e3.

20. Chipman SD, Sweet HO, McBride DJ et al. 1993. Defective pro alpha 2 (i) collagen synthesis in a recessive mutation in mice: A model of human osteogenesis imperfecta. Proceedings of the National Academy of Sciences. 90(5):1701-1705.

21. Saban J, Zussman M, Havey R et al. 1996. Heterozygous oim mice exhibit a mild form of osteogenesis imperfecta. Bone. 19(6):575-579.

22. McBride Jr D, Shapiro J, Dunn M. 1998. Bone geometry and strength measurements in aging mice with the oim mutation. Calcif Tissue Int. 62(2):172-176.

23. Phillips CL, Bradley DA, Schlotzhauer CL et al. 2000. oim mice exhibit altered femur and incisor mineral composition and decreased bone mineral density. Bone. 27(2):219-226.

24. Bart ZR, Hammond MA, Wallace JM. 2014. Multi-scale analysis of bone chemistry, morphology and mechanics in the oim model of osteogenesis imperfecta. Connect Tissue Res. 55(sup1):4-8.

25. Gentry BA, Ferreira AJ, McCambridge AJ, Brown M, Phillips CL. 2010. Skeletal muscle weakness in osteogeneis imperfecta mice. Matrix Biol. 29(7):638-644.

26. Carleton SM, McBride DJ, Carson WL et al. 2008. Role of genetic background in determining phenotypic severity throughout postnatal development and at peak bone mass in col1a2 deficient mice (oim). Bone. 42(4):681-694.

27. Bouxsein ML, Boyd SK, Christiansen BA et al. 2010. Guidelines for assessment of bone microstructure in rodents using micro–computed tomography. J Bone Miner Res. 25(7):1468-1486.

28. Vanleene M, Porter A, Guillot P-V et al. 2012. Ultra-structural defects cause low bone matrix stiffness despite high mineralization in osteogenesis imperfecta mice. Bone. 50(6):1317-1323.

29. Miller E, Delos D, Baldini T, Wright TM, Camacho NP. 2007. Abnormal mineral-matrix interactions are a significant contributor to fragility in oim/oim bone. Calcif Tissue Int. 81(3):206-214.

30. Yao X, Carleton SM, Kettle AD et al. 2013. Gender-dependence of bone structure and properties in adult osteogenesis imperfecta murine model. Ann Biomed Eng. 41(6):1139-1149.

31. Caudill A, Flanagan A, Hassani S et al. 2010. Ankle strength and functional limitations in children and adolescents with type i osteogenesis imperfecta. Pediatr Phys Ther. 22(3):288-295.

32. Pavone V, Mattina T, Pavone P, Falsaperla R, Testa G. 2017. Early motor delay: An outstanding, initial sign of osteogenesis imperfecta type 1. Journal of orthopaedic case reports. 7(3):63-66.

33. Boot AM, De Coo RF, Pals G, de Muinck Keizer-Schrama SM. 2006. Muscle weakness as presenting symptom of osteogenesis imperfecta. Eur J Pediatr. 165(6):392-394.

34. Oestreich A, Carleton S, Yao X et al. 2016. Myostatin deficiency partially rescues the bone phenotype of osteogenesis imperfecta model mice. Osteoporos Int. 27(1):161-170.

35. DiGirolamo DJ, Singhal V, Chang X, Lee S-J, Germain-Lee EL. 2015. Administration of soluble activin receptor 2b increases bone and muscle mass in a mouse model of osteogenesis imperfecta. Bone research. 3:14042.

36. De Souza RL, Matsuura M, Eckstein F et al. 2005. Non-invasive axial loading of mouse tibiae increases cortical bone formation and modifies trabecular organization: A new model to study cortical and cancellous compartments in a single loaded element. Bone. 37(6):810-818.

37. Landis WJ. 1995. Tomographic imaging of collagen-mineral interaction: Implications for osteogenesis imperfecta. Connect Tissue Res. 31(4):287-290.

38. Landis WJ. 1995. The strength of a calcified tissue depends in part on the molecular structure and organization of its constituent mineral crystals in their organic matrix. Bone. 16(5):533-544.

39. Misof K, Landis WJ, Klaushofer K, Fratzl P. 1997. Collagen from the osteogenesis imperfecta mouse model (oim) shows reduced resistance against tensile stress. The Journal of clinical investigation. 100(1):40-45.

40. McBride DJ, Choe V, Shapiro JR, Brodsky B. 1997. Altered collagen structure in mouse tail tendon lacking the α2(i) chain. J Mol Biol. 270(2):275-284.

41. Sims T, Miles C, Bailey A, Camacho N. 2003. Properties of collagen in oim mouse tissues. Connect Tissue Res. 44(1):202-205.

42. Brotto M, Bonewald L. 2015. Bone and muscle: Interactions beyond mechanical. Bone. 80:109-114.

43. Brotto M, Johnson ML. 2014. Endocrine crosstalk between muscle and bone. Current Osteoporosis Reports. 12(2):135-141.

44. Phillips CL, Jeong Y. 2018. Osteogenesis imperfecta: Muscle–bone interactions when bi-directionally compromised. Current osteoporosis reports.1-12.

Figure Legends:

Figure 1: Example torque (A-C) and strain (D-F) curves during muscle stimulation of WT, Het, and oim/oim at 25 Hz (A,D), 50 Hz (B,E), and 150 Hz (C,F) stimulation frequency. Note tetanic muscle contraction occurred by 150 Hz.

Figure 2: Functional and area-based muscle analysis indicated significant muscle weakness in oim/oim, but not Het. A) Frequency-based analysis showed reduced maximum torque in oim/oim at all but the lowest stimulation frequency (25 Hz). B) Maximum torque at a single frequency (150 Hz) further demonstrates this reduction. C) Interestingly, we also noticed that the rising torque-time slope was reduced, with oim/oim having the shallowest slope and Het having an intermediate slope. D) CT analysis of muscle area also indicated muscle weakness in oim/oim. In panel A, "&" indicates comparison between WT and oim/oim and "#' between Het and oim/oim ($p<0.001$ for both). In panels B-D, *$p<0.05$, **$p<0.01$, ***$p<0.001$ with the bars showing comparisons.

Figure 3: Example cortical micro-CT images at the mid-diaphysis of A) WT, B) Het, and C) oim/oim. Oim/oim had smaller bones as indicated by D) reduced cross-sectional area, E) marrow area, G) periosteal bone surface and H) endocortical bone surface. F) Together, these resulted in a reduced cross-sectional maximum moment of inertia, suggesting that oim/oim bones have reduced resistance to bending. I) Tissue mineral density was increased in oim/oim. White scale bars: 0.5 mm. *$p<0.05$, **$p<0.01$, ***$p<0.001$ with the bars showing comparisons.

Figure 4: A) Maximum strain was reduced in oim/oim at stimulation frequencies greater than 50 Hz. B) Maximum strain at a single frequency (150 Hz) further demonstrates this reduction. C) After normalizing strain to torque, oim/oim showed higher strain relative to toque at all frequency, and D) further demonstrated at 150 Hz. E) Similarly, grouping all frequencies and all

mice of a genotype together also demonstrates a higher strain vs torque slope in oim/oim. In panels A and C, “&” indicates comparison between WT and oim/oim and “#” between Het and oim/oim. In panels B and D, *p<0.05, **p<0.01, ***p<0.001 with the bars showing comparisons.

Figure 5: Micro-CT image showing calcified tendon and broken calcaneus. The percentage of each genotype with either a calcified tendon or broken calcaneus are also shown.

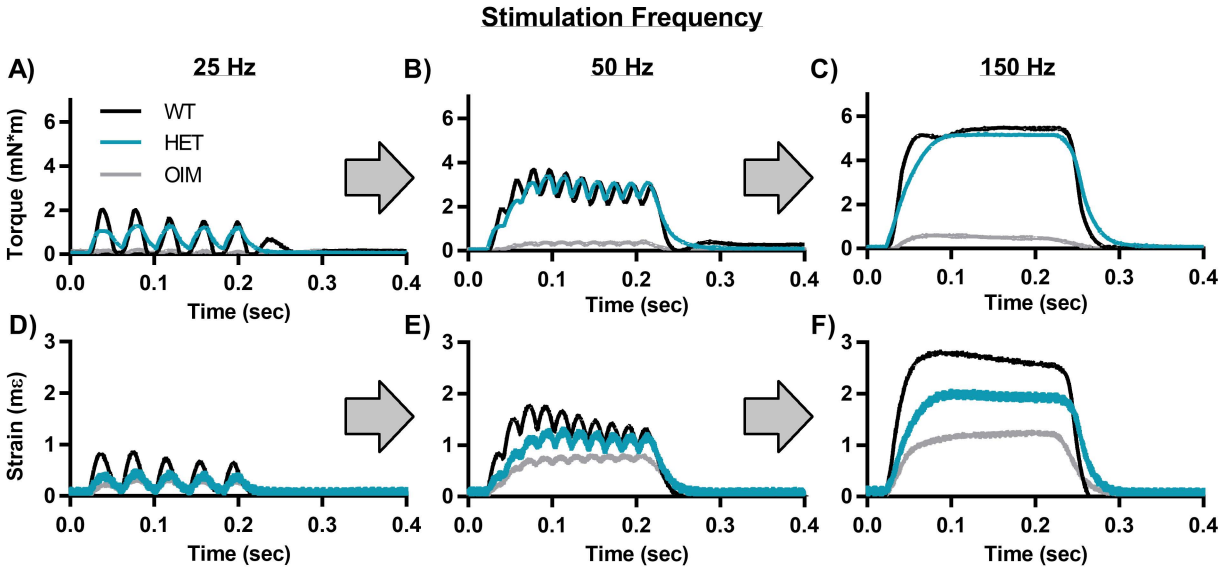
Stimulation Frequency
A)
25 Hz
B)
50 Hz
C)
150 Hz
WT
HET
OIM
Torque (mN*m)
Time (sec)
D)
E)
F)
Strain (mε)
Time (sec)

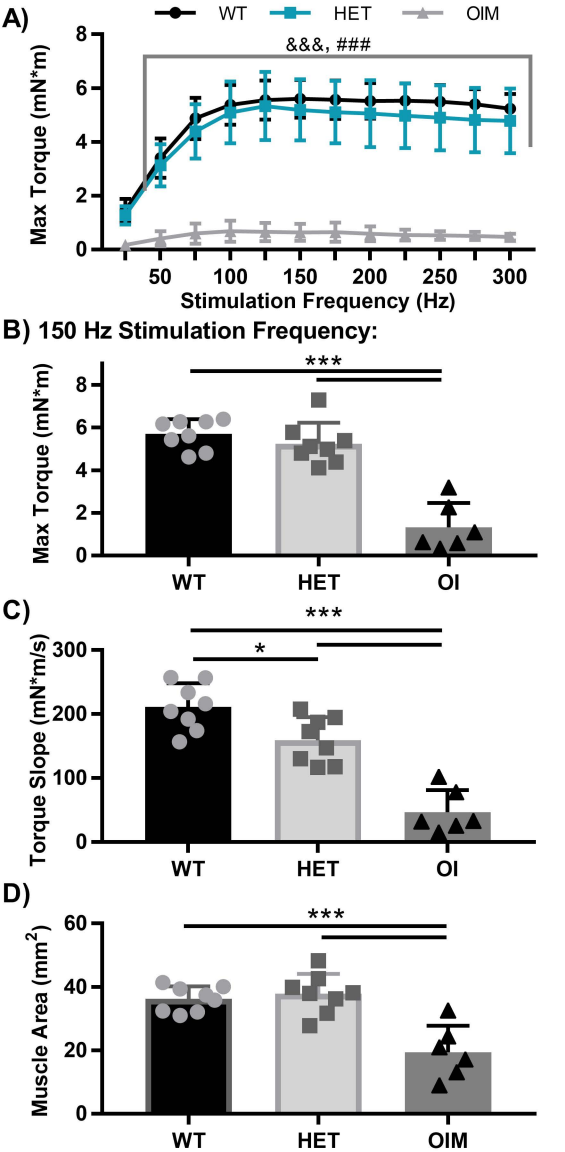
A)
WT
HET
OIM
&&&, ###
Max Torque (mN*m)
Stimulation Frequency (Hz)
B) 150 Hz Stimulation Frequency:
***
Max Torque (mN*m)
WT
HET
OI
C)
***
*
Torque Slope (mN*m/s)
WT
HET
OI
D)
***
Muscle Area (mm2)
WT
HET
OIM

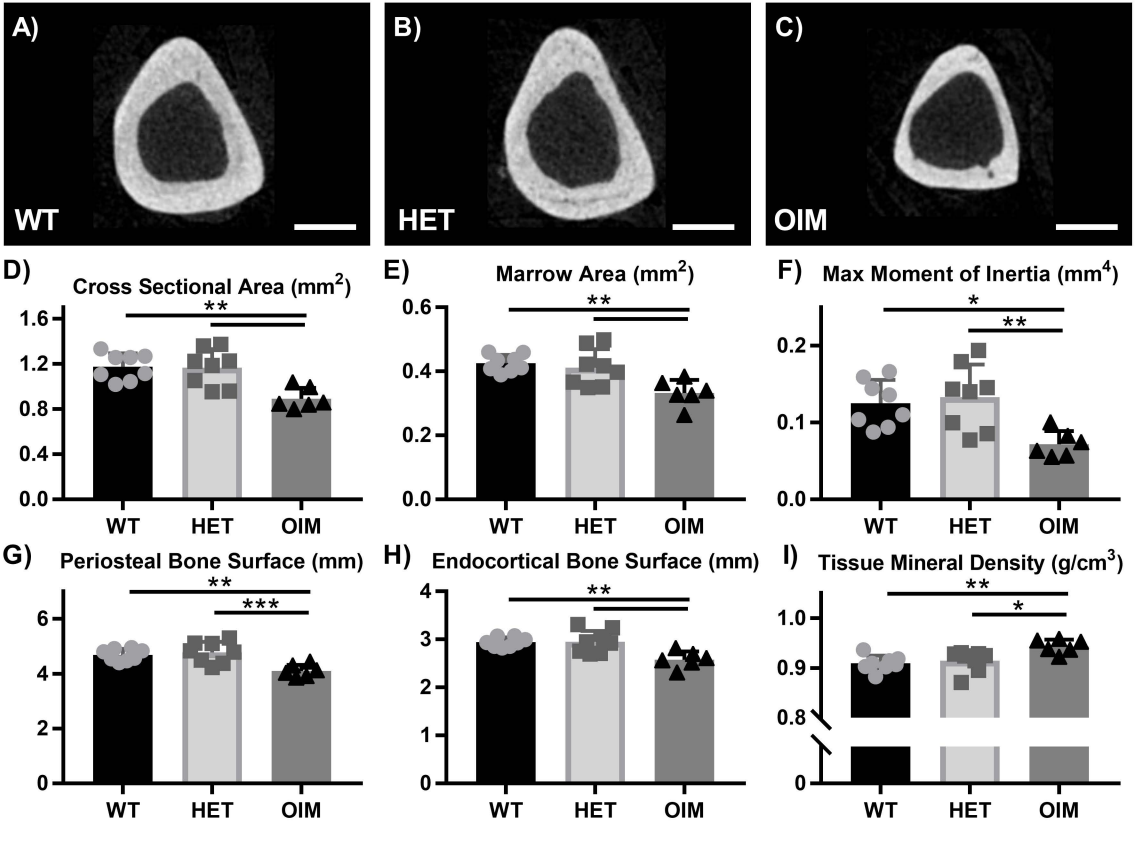
A)
WT
B)
HET
C)
OIM
D)
Cross Sectional Area (mm2)
**
1.6
1.2
0.8
0.4
0.0
WT
HET
OIM
E)
Marrow Area (mm2)
**
0.6
0.4
0.2
0.0
WT
HET
OIM
F)
Max Moment of Inertia (mm4)
*
**
0.2
0.1
0.0
WT
HET
OIM
G)
Periosteal Bone Surface (mm)
**
***
6
4
2
0
WT
HET
OIM
H)
Endocortical Bone Surface (mm)
**
4
3
2
1
0
WT
HET
OIM
I)
Tissue Mineral Density (g/cm3)
**
*
1.0
0.9
0.8
0
WT
HET
OIM

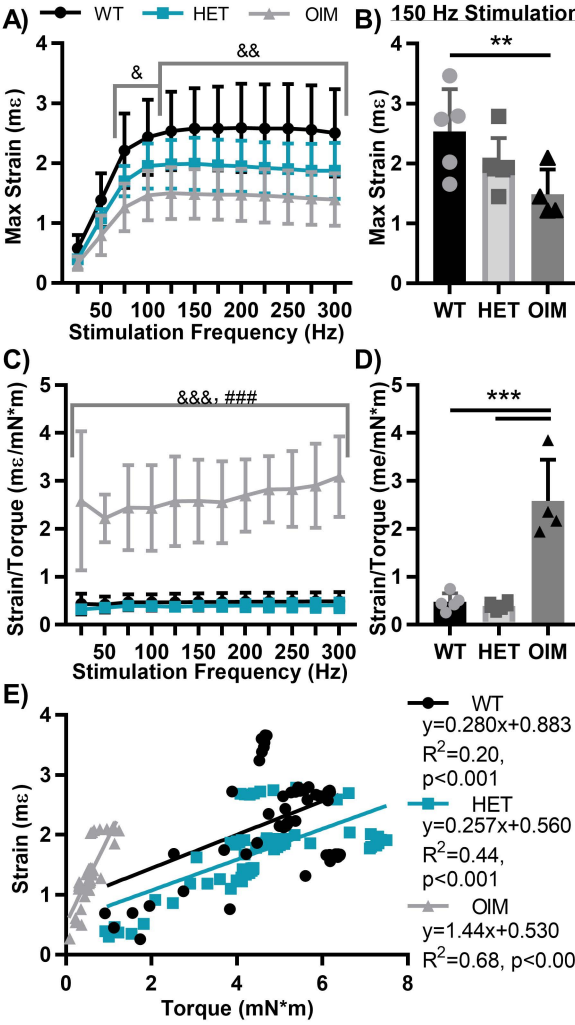
A)
WT
HET
OIM
Max Strain (mε)
&
&&
Stimulation Frequency (Hz)
B)
150 Hz Stimulation
**
Max Strain (mε)
WT HET OIM
C)
&&&, ###
Strain/Torque (mε/mN*m)
Stimulation Frequency (Hz)
D)
***
Strain/Torque (me/mN*m)
WT HET OIM
E)
Strain (mε)
Torque (mN*m)
WT
y=0.280x+0.883
R2=0.20,
p<0.001
HET
y=0.257x+0.560
R2=0.44,
p<0.001
OIM
y=1.44x+0.530
R2=0.68, p<0.001

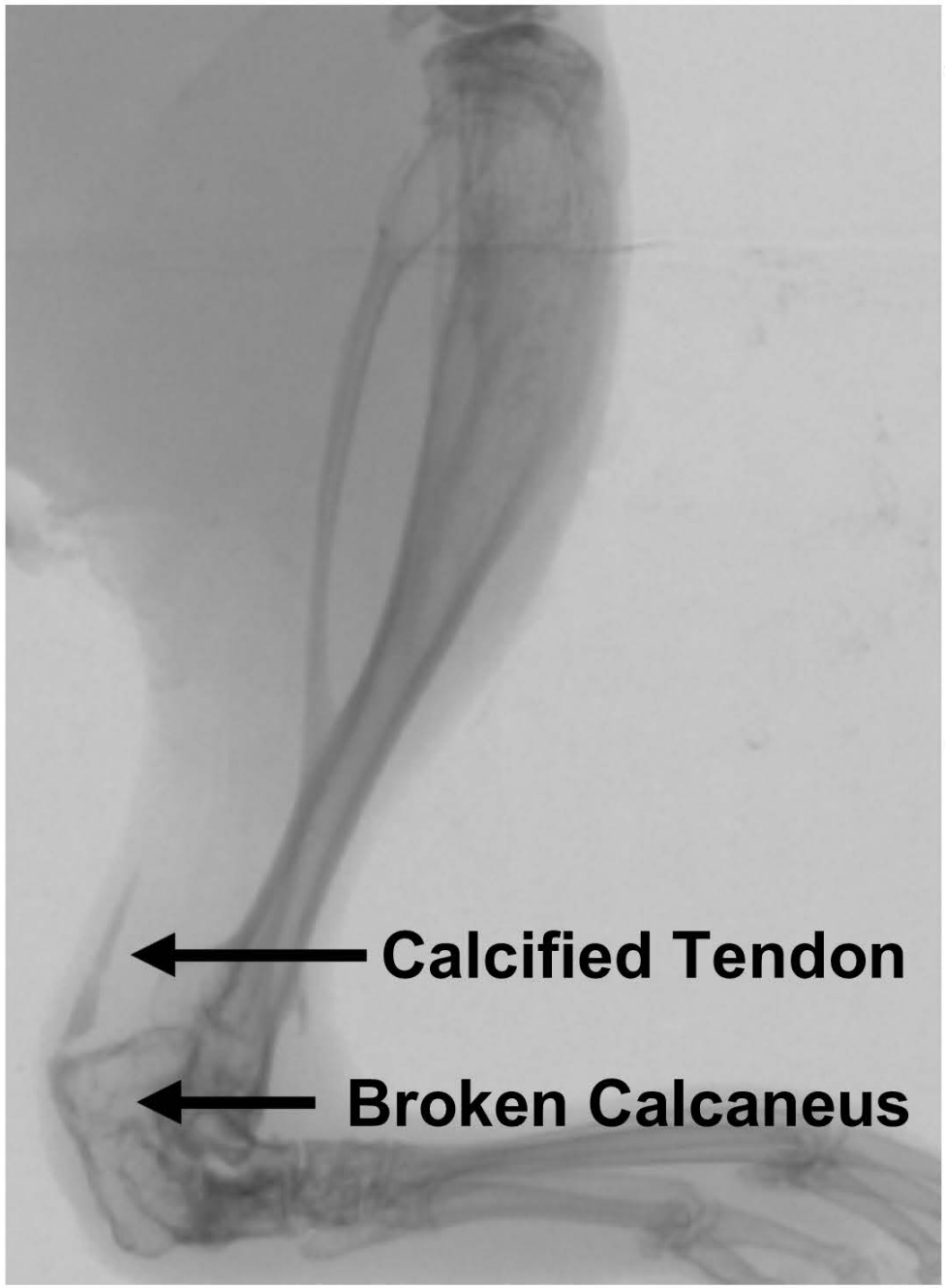
Calcified Tendon
Broken Calcaneus

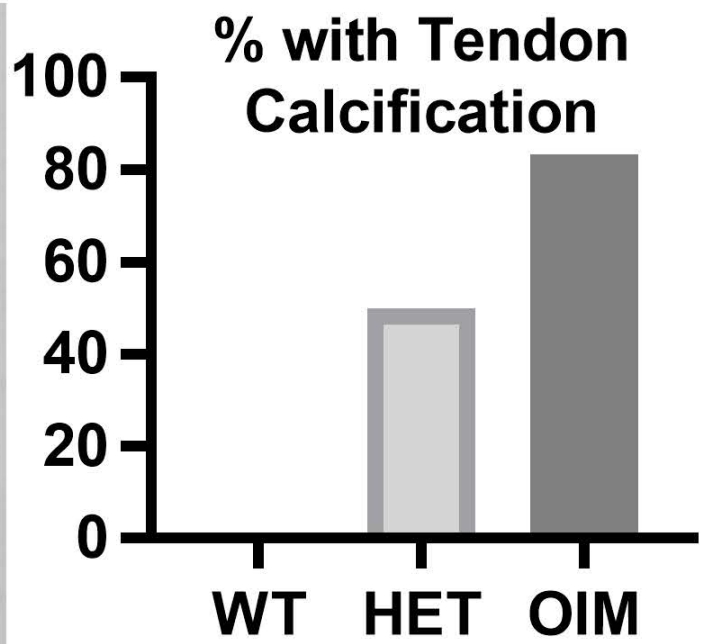
% with Tendon Calcification
100
80
60
40
20
0
WT
HET
OIM

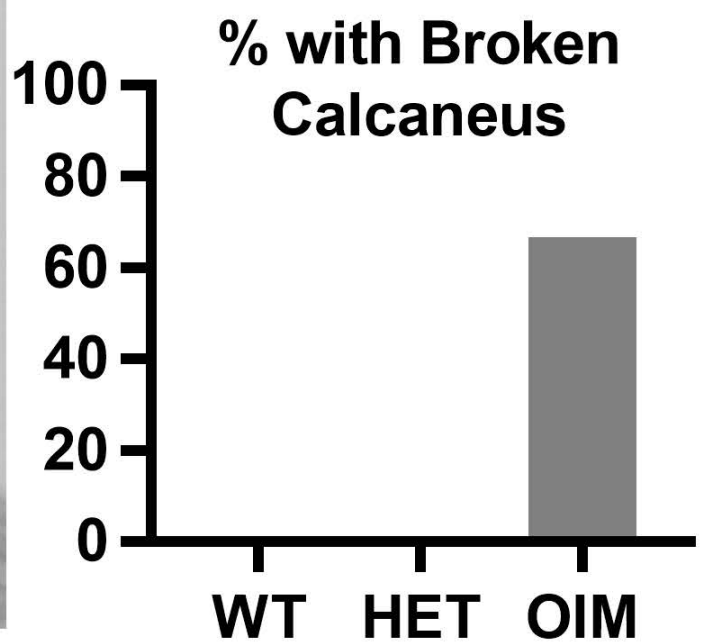
% with Broken Calcaneus
100
80
60
40
20
0
WT
HET
OIM